Episodic Dust Events of Utah's Wasatch Front and Adjoining Region

W. JAMES STEENBURGH AND JEFFREY D. MASSEY

Department of Atmospheric Sciences, University of Utah, Salt Lake City, Utah

THOMAS H. PAINTER

Jet Propulsion Laboratory, Pasadena, California

(Manuscript received 4 January 2012, in final form 4 April 2012)

ABSTRACT

Episodic dust events cause hazardous air quality along Utah's Wasatch Front and dust loading of the snowpack in the adjacent Wasatch Mountains. This paper presents a climatology of episodic dust events of the Wasatch Front and adjoining region that is based on surface weather observations from the Salt Lake City International Airport (KSLC), Geostationary Operational Environmental Satellite (GOES) imagery, and additional meteorological datasets. Dust events at KSLC—defined as any day [mountain standard time (MST)] with at least one report of a dust storm, blowing dust, and/or dust in suspension with a visibility of 10 km or less—average 4.3 per water year (WY: October–September), with considerable interannual variability and a general decline in frequency during the 1930–2010 observational record. The distributions of monthly dust-event frequency and total dust flux are bimodal, with primary and secondary maxima in April and September, respectively. Dust reports are most common in the late afternoon and evening. An analysis of the 33 most recent (2001–10 WY) events at KSLC indicates that 11 were associated with airmass convection, 16 were associated with a cold front or baroclinic trough entering Utah from the west or northwest, 4 were associated with a stationary or slowly moving front or baroclinic trough west of Utah, and 2 were associated with other synoptic patterns. GOES imagery from these 33 events, as well as 61 additional events from the surrounding region, illustrates that emission sources are located primarily in low-elevation Late Pleistocene–Holocene alluvial environments in southern and western Utah and southern and western Nevada.

1. Introduction

Dust storms have an impact on air quality (Pope et al. 1995; Gebhart et al. 2001), precipitation (Goudie and Middleton 2001), soil erosion (Gillette 1988; Zobeck et al. 1989), the global radiation budget (Ramanathan et al. 2001), and regional climate (Nicholson 2000; Goudie and Middleton 2001). Recent research examining dust-related radiative forcing of the mountain snowpack of western North America and other regions of the world has initiated a newfound interest in dust research (Painter et al. 2007; Flanner et al. 2009; Painter et al. 2010). For example, observations from Colorado's San Juan Mountains indicate that dust loading increases the snowpack's absorption of solar radiation, decreasing seasonal snow-cover duration by several weeks (Painter et al. 2007). Modeling studies further suggest that radiative forcing from increased dust deposition during the past 150 years results in an earlier runoff with reduced annual volume in the upper Colorado River Basin (Painter et al. 2010).

Synoptic and mesoscale weather systems are the primary drivers of global dust emissions and transport. Mesoscale convective systems that propagate eastward from Africa over the Atlantic Ocean produce one-half of the dust emissions from the Sahara Desert, the world's largest aeolian dust source (Swap et al. 1996; Goudie and Middleton 2001). Dust plumes generated by these systems travel for several days in the large-scale easterly flow (Carlson 1979), with human health and ecological impacts across the tropical Atlantic and Caribbean Sea (Goudie and Middleton 2001; Prospero and Lamb 2003). In northeastern Asia, strong winds in

Corresponding author address: Dr. W. James Steenburgh, Dept. of Atmospheric Sciences, University of Utah, 135 South 1460 East, Rm. 819, Salt Lake City, UT 84112.
E-mail: jim.steenburgh@utah.edu

DOI: 10.1175/JAMC-D-12-07.1

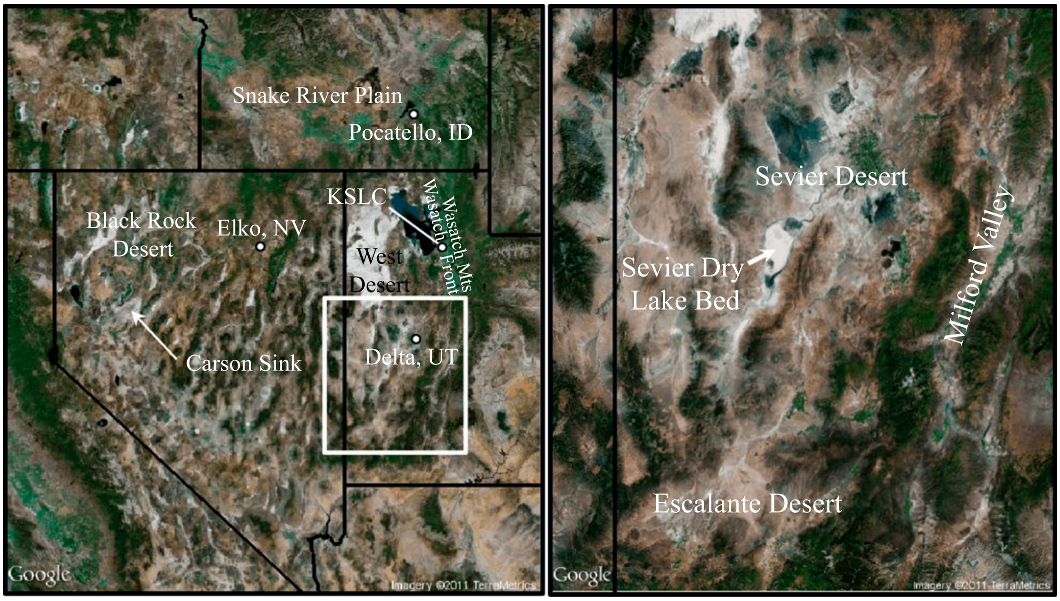

FIG. 1. Google Earth image of the Intermountain West with geographic features that are discussed in the text annotated. The inset box in the left panel shows the location of the right panel, which encompasses the Sevier Desert, Sevier Dry Lake Bed, Escalante Desert, and Milford Valley region. [©2011 Google; imagery ©2011 TerraMetrics.]

the post-cold-frontal environment of Mongolian cyclones drive much of the dust emissions (Yasunori and Masao 2002; Shao and Wang 2003; Qian et al. 2002). The highest frequency of Asian dust storms occurs over the Taklimakan and Gobi Deserts of northern China, where dust is observed 200 days yr^{-1} (Qian et al. 2002). Fine dust from these regions can be transported to the United States, producing aerosol concentrations that are above National Ambient Air Quality Standards (Jaffe et al. 1999; Husar et al. 2001; VanCuren and Cahill 2002; Fairlie et al. 2007).

In North America, the Great Basin, Colorado Plateau, and Mojave and Sonoran Deserts produce most of the dust emissions (Reynolds et al. 2001; Tanaka and Chiba 2006; see Fig. 1 for geographic and topographic locations). Desert land surfaces are naturally resistant to wind erosion because of the presence of physical, biological, and other crusts (Gillette et al. 1980) but are easily disturbed, in some cases leading to increased dust emissions long after the initial disturbance (e.g., Belnap et al. 2009). From alpine lake sediments collected over the interior western United States, Neff et al. (2008) and Reynolds et al. (2010) find dramatically larger dust deposition rates since the mid–nineteenth century, a likely consequence of land surface disturbance by livestock grazing, plowing of agricultural soils, and other human activities.

Several studies suggest that the synoptic and mesoscale weather systems that generate dust emissions and transport over western North America vary geographically and seasonally. Orgill and Sehmel (1976) identified a spring maximum in suspended dust frequency over the contiguous United States as a whole, which they attributed to cyclonic and convective storm activity, but found that some locations in the Pacific Coast and Rocky Mountain regions have an autumn maximum. Brazel and Nickling (1986, 1987) found that fronts, thunderstorms, cutoff lows, and tropical disturbances (i.e., decaying tropical depressions and cyclones originating over the eastern Pacific Ocean) are the primary drivers of dust emissions in Arizona. The frequency of dust emissions from fronts is highest from late autumn to spring, that from thunderstorms is highest during the summer, and that from cutoff lows is highest from May to June and from September to November. Dust emissions produced by tropical disturbances are infrequent but are likely confined to June–October during which tropical cyclone remnants move across the southwestern United States (Ritchie et al. 2011). For dust events in nearby California and southern Nevada, Changery (1983) and Brazel and Nickling (1987) established linkages with frontal passages and cyclone activity, respectively, with land surface conditions (e.g., soil moisture and vegetation) affecting dust-event seasonality and spatial distribution. In northwestern Nevada, dust storms originating over the Black Rock Desert have been linked to strong winds associated with cold-frontal passages and geostrophic adjustment, with

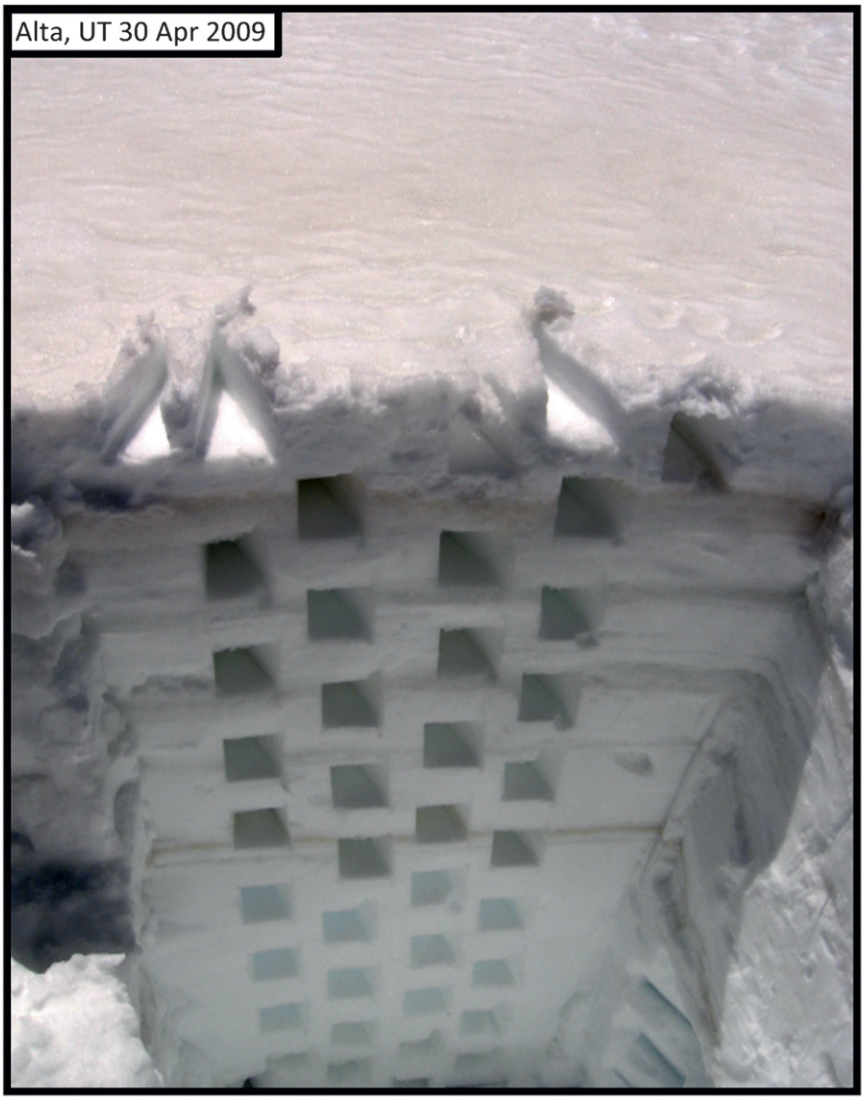

FIG. 2. A snowpit from Alta, Utah, on 30 Apr 2009 that exhibits dust layers from episodic dust events.

emissions being strongly dependent on antecedent rainfall and soil conditions (Lewis et al. 2011; Kaplan et al. 2011).

Episodic dust events of Utah's Wasatch Front and adjoining region produce hazardous air quality in the Salt Lake City, Utah, metropolitan area and dust loading of the snowpack in the Wasatch Mountains (Fig. 2). From 2002 to 2010 in Utah, wind-blown dust events contributed to 13 exceedances of the National Ambient Air Quality Standard for particulate matter of less than 2.5 (PM2.5) or 10 (PM10) μm in diameter (T. Cruickshank, Utah Division of Air Quality, 2011, personal communication). Dust loading in the Wasatch Mountains affects a snowpack that serves as the primary water resource for approximately 400 000 people and enables a $1.2 billion winter sports industry, known internationally for the ''Greatest Snow on Earth'' (Bear West Consulting Team 1999; Steenburgh and Alcott 2008; Gorrell 2011).

This paper examines the climatological characteristics (or ''climatology'') of episodic dust events of the Wasatch Front and adjoining region. The available meteorological data illustrate that dust events occur throughout the historical record and that they are associated primarily with synoptic cold fronts, baroclinic troughs (i.e., a pressure trough with a modest temperature gradient that is insufficiently strong to be called a front; Sanders 1999), and airmass convection. Emission sources are located primarily in low-elevation Late Pleistocene–Holocene alluvial environments in southern and western Utah and southern and western Nevada.

2. Data and methods

a. Long-term climatology

Our long-term dust-event climatology derives from hourly surface weather observations from the Salt Lake City International Airport (KSLC), which we obtained from the Global Integrated Surface Hourly Database (DS-3505) at the National Climatic Data Center (NCDC). KSLC is located in the Salt Lake Valley just west of downtown Salt Lake City and the Wasatch Mountains (Fig. 1) and provides the longest quasi-continuous record of hourly weather observations in northern Utah. The analysis covers the 1930–2010 water years (October–September) when 97.9% of all possible hourly observations are available.[1]

The hourly weather observations included in DS-3505 derive from multiple sources, with decoding and processing occurring at either operational weather centers or the Federal Climate Complex in Asheville, North Carolina (Lott et al. 2001; NCDC 2008). Studies of dust events frequently use similar datasets (e.g., Orgill and Sehmel 1976; Hall 1981; Changery 1983; Nickling and Brazel 1984; Brazel and Nickling 1986, 1987; Brazel 1989; Qian et al. 2002; Yasunori and Masao 2002; Shao and Wang 2003; Shao et al. 2003; Song et al. 2007). Nevertheless, although hourly weather observations are useful for examining the general climatological and meteorological characteristics of dust events, they do not quantify dust concentrations, making the identification and classification of dust somewhat subjective. Inconsistencies arise from observer biases, changes in instrumentation, reporting guidelines, and processing algorithms. These inconsistencies result in the misreporting of some events (e.g., dust erroneously reported as haze) and limit confident assessment and interpretation of long-term trends and variability.

Consistent with World Meteorological Organization (WMO) guidelines (WMO 2009), the present-weather record in DS-3505 includes 11 dust categories (Table 1). During the study period, there were 916 reports of blowing dust (category 7), 178 of dust in suspension (category 6), 7 of dust storm (categories 9, 30–32, and 98), and 1 of dust or sand whirl (category 8) at KSLC. There were no reports of severe dust storm (categories 33–35). Among the reports of blowing dust, dust in suspension, and dust storm, there were 69 with a visibility of greater than 6 statute mi (10 km), the threshold currently used by the WMO and national weather agencies for reporting blowing dust or dust in suspension (Shao et al. 2003; OFCM 2005). Because these events are weak or may be erroneous, they were removed from the analysis. They include all but one of the seven dust-storm reports. The report of dust or sand whirl was also removed because we are interested in widespread events rather than localized dust whirl(s) (also called "dust devils"). The resulting long-term dust-event climatology is based on the remaining 1033 reports. A dust event is any day [mountain standard time (MST)] with at least one such dust report.

b. Synoptic classification of recent dust events

Our analysis of the synoptic conditions contributing to Wasatch Front dust events concentrates on events at KSLC during the most recent 10-yr period (2001–10). This enables the use of modern satellite and reanalysis data and limits the number of events, making the synoptic classification of each event feasible.

Resources used in our manual analysis to subjectively classify dust events and prepare case studies include the North American Regional Reanalysis (NARR), Geostationary Operational Environmental Satellite (GOES) imagery, Salt Lake City (KMTX) radar imagery, and hourly KSLC surface weather observations and remarks from DS-3505. The NARR is a 32-km, 45-layer reanalysis for North America that is based on the National Centers for Environmental Predication (NCEP) Eta Model and data assimilation system (Mesinger et al. 2006). Relative to the European Centre for Medium-Range Weather Forecasts Interim Re-Analysis (ERA-Interim) and NCEP–National Center for Atmospheric Research (NCAR) reanalysis, the NARR better resolves the complex terrain of the Intermountain West but still has a poor representation of the basin-and-range topography over Nevada (Jeglum et al. 2010). We obtained the NARR data from the National Oceanic and Atmospheric Administration (NOAA) Operational Model Archive Distribution System (NOMADS) at NCDC (online at http://nomads.ncdc.noaa.gov/#narr_datasets), the level-II KMTX radar data from NCDC (online at http://www.ncdc.noaa.gov/nexradinv/), and the GOES data from the NOAA Comprehensive Large Array–Data Stewardship System (CLASS; online at http://www.class.ncdc.noaa.gov).

c. Dust emission sources

We identify dust emission sources during 2001–10 using a dust-retrieval algorithm applied to GOES data. Because the algorithm only works in cloud-free areas and many dust events occur in conjunction with cloud cover, we expand the number of events to include those

[1] Hereinafter, all years in this paper are water years.

TABLE 1. The DS-3505 dust-related present-weather categories, along with full and abbreviated descriptions (the latter are used in the text), total number of reports, and number of reports used in the analysis (in parentheses).

Category	Full description	Abbreviated description used in text	Total reports (reports used in analysis)
06	Widespread dust in suspension in the air, not raised by wind at or near the station at the time of observation	Dust in suspension	178 (155)
07	Dust or sand raised by wind at or near the station at the time of observation, but no well-developed dust whirl(s) or sand whirl(s), and no duststorm or sandstorm seen	Blowing dust	916 (877)
08	Well-developed dust whirl(s) or sand whirl(s) seen at or near the station during the preceding hour or at the time of observation, but no duststorm or sandstorm	Dust whirl(s)	1 (0)
09	Duststorm or sandstorm within sight at the time of observation, or at the station during the preceding hour	Duststorm	2(1)
30	Slight or moderate duststorm or sandstorm has decreased during the preceding hour	Duststorm	1 (0)
31	Slight or moderate duststorm or sandstorm no appreciable change during the preceding hour	Duststorm	1 (0)
32	Slight or moderate duststorm or sandstorm has begun or has increased during the preceding hour	Duststorm	1 (0)
33	Severe duststorm or sandstorm has decreased during the preceding hour	Duststorm	0 (0)
34	Severe duststorm or sandstorm no appreciable change during the preceding hour	Duststorm	0 (0)
35	Severe duststorm or sandstorm has begun or has increased during the preceding hour	Duststorm	0 (0)
98	Thunderstorm combined with duststorm or sandstorm at time of observation, thunderstorm at time of observation	Duststorm	2 (0)

identified in 1) DS-3505 reports from stations in the surrounding region with at least 5 years of hourly data [Delta, Utah (KU24); Elko, Nevada (KEKO); and Pocatello, Idaho (KPIH); see Fig. 1]; 2) the authors' personal notes, which derive from weather analysis over the past several years and include events identified visually in the Salt Lake Valley or using satellite imagery from the surrounding region; and 3) Utah Avalanche Center annual reports. This analysis is thus not specific to KSLC but does identify emissions sources that contribute to dust events in the region.

The dust-retrieval algorithm is a modified version of that used by Zhao et al. (2010, p. 2349) to detect dust over land with Moderate Resolution Imaging Spectroradiometer (MODIS) data, which uses brightness temperature T_b from three infrared channels (3.9, 11, and 12 μm) and reflectance from four visible channels (0.47, 0.64, 0.86, and 1.38 μm). GOES has three corresponding infrared channels (3.9, 10.7, and 12 μm) but only one visible channel (0.65 μm). Therefore, we use an albedo of 0.25 or greater in the 0.65-μm visible channel to screen for clouds. Then, we substitute the GOES 10.7-μm channel for the MODIS 11-μm channel and identify the existence of dust if $T_b(3.9\ \mu\text{m}) \leq T_b(10.7\ \mu\text{m})$ and $T_b(10.7\ \mu\text{m}) - 10\ \text{K} \geq T_b\ (12\ \mu\text{m})$. These thresholds are slightly modified from those used

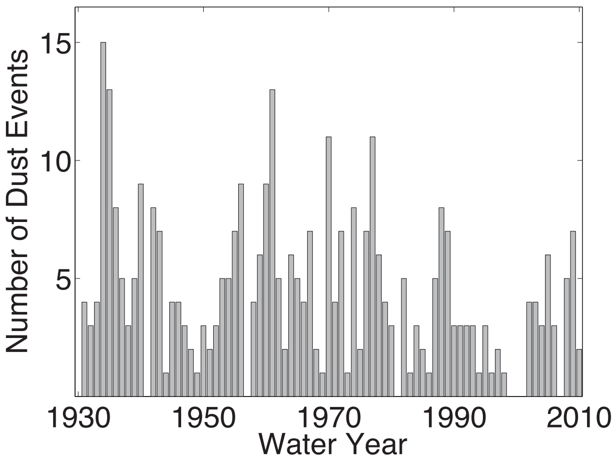

FIG. 3. Number of dust events at KSLC by water year.

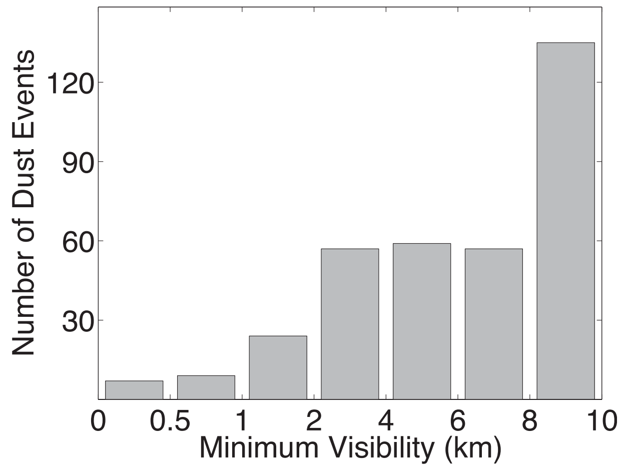

FIG. 4. Minimum visibility (km) during KSLC dust events.

by Zhao et al. (2010) and were selected through experimentation and comparison with dust detected visually and using the Zhao et al. (2010) technique applied to MODIS imagery from several events. Because uncertainties arise when the sun angle is low and when dust is near cloud edges, the algorithm is applied approximately every 15 min during the daylight hours (0700–1900 MST), with plume origin and orientation identified subjectively. Because the footprint of the GOES infrared channels is 4 km and the algorithm fails to identify shallow dust (Zhao et al. 2010), the plume origin is approximate.

3. Results

a. Long-term climatology

Dust events at KSLC occur throughout the historical record, with an average of 4.3 per water year (Fig. 3). Considerable interannual variability exists, with no events reported in seven years (1941, 1957, 1981, 1999, 2000, 2001, and 2007) and a maximum of 15 in 1934. No effort was made to quantify or assess long-term trends or interdecadal/interannual variability given the subjective nature of the reports and changes in observers, observing methods, and instrumentation during the study period. The general decline in dust-event frequency, however, is broadly consistent with a decrease in mass accumulation rates related to dust deposition in alpine lakes of western Colorado following the passage of the Taylor Grazing Act of 1934 (Neff et al. 2008).

On the basis of current weather-observing practices (Glickman 2000; Shao and Wang 2003), the minimum visibility when dust is reported meets the criteria for blowing dust [1 km (5/8 statute mi) < visibility ≤ 10 km (6 statute mi)], a dust storm [0.5 km (5/16 statute mi) < visibility ≤ 1 km (5/8 statute mi)], or a severe dust storm [visibility ≤ 0.5 km (5/16 statute mi)] in 95.4%, 2.6%, and 2.0% of the dust events, respectively (Fig. 4).[2] Therefore, only a small fraction of the dust events and observations meet the criteria for dust storm or severe dust storm.

To integrate the effects of KSLC event severity, frequency, and duration, we first estimate the dust concentration C (μg m^{-3}), for each dust report following Eqs. (6) and (7) of Shao et al. (2003):

$$C = 3802.29D_v^{-0.84} \quad D_v < 3.5\,\text{km} \quad \text{and}$$

$$C = \exp(-0.11D_v + 7.62) \quad D_v \geq 3.5\,\text{km},$$

where D_v is the visibility. Multiplying C by the sustained wind speed (currently a 2-min average, although the averaging period may have varied during the observational record) yields the scalar dust flux, which after time integration yields an estimate for the total dust flux during the period of interest. On an annual basis, the total dust flux averages 399.4 g m^{-2}, with a maximum of 2810.2 g m^{-2} in 1935 (Fig. 5). Because it integrates event severity, frequency, and duration, the annual total dust flux provides a somewhat different perspective from the annual number of dust events (cf. Figs. 3 and 5). For example, 1934 featured the most dust events, but the greatest total dust flux occurred in 1935. In 2010, there were only two dust events, but they were major events that produced a decadal-scale maximum in total dust flux. Nevertheless, the annual total dust flux exhibits an overall decline, similar to event frequency.

[2] The visibility observations are taken and stored in statute miles, but approximate metric thresholds are used hereinafter.

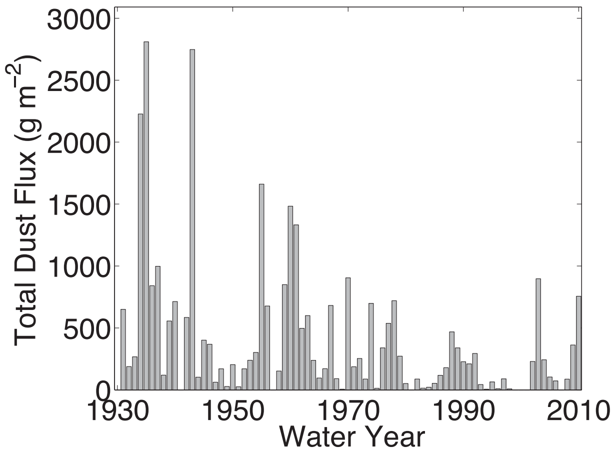

FIG. 5. Total dust flux during KSLC dust events by water year.

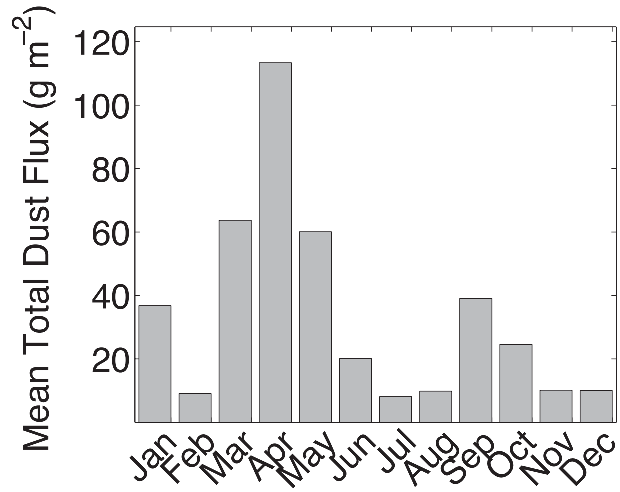

FIG. 7. Mean monthly total dust flux during KSLC dust events.

The monthly distribution of dust events is bimodal, with primary and secondary peaks in April and September, respectively (Fig. 6). Similar peaks are observed in the mean monthly total dust flux, but with an additional peak in January (Fig. 7). This January peak is surprising, but it results primarily from an unusually strong multiday event in January of 1943 that contributed to 83% of the January monthly mean. In the summer, the mean monthly near-surface minimum is distinctly lower relative to the dust-event frequency (cf. Figs. 6 and 7), suggesting that summer dust events are shorter and weaker. For March–May, which usually encompasses the climatological peak in snowpack snow water equivalent and the onset of the spring runoff, the mean monthly total dust flux is 237 g m^{-2}, or 59% of the mean annual total dust flux.

Similar bimodal or modal distributions with a primary or single spring dust peak have been identified in the Taklimakan desert of China (Yasunori and Masao 2002), southern Great Plains of the United States (Stout 2001), Mexico City, Mexico (Jauregui 1989), and the Canadian prairies (Wheaton and Chakravarti 1990). The spring peak appears to be the result of a high frequency of wind events driven by cyclones and fronts passing over a recently dried, erodible land surface. Indeed, the bimodal distributions of dust events and mean monthly total dust flux at KSLC are very similar to that of cold fronts and cyclones in the Intermountain West, which are strongest and most frequent in the spring and have a secondary peak in the autumn (Shafer and Steenburgh 2008; Jeglum et al. 2010). These cold fronts and cyclones produce persistently strong winds that have been implicated in sand transport and dune

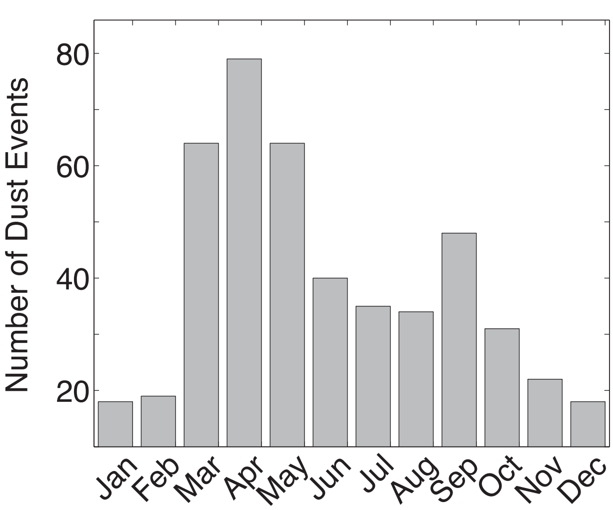

FIG. 6. Number of dust events at KSLC by month.

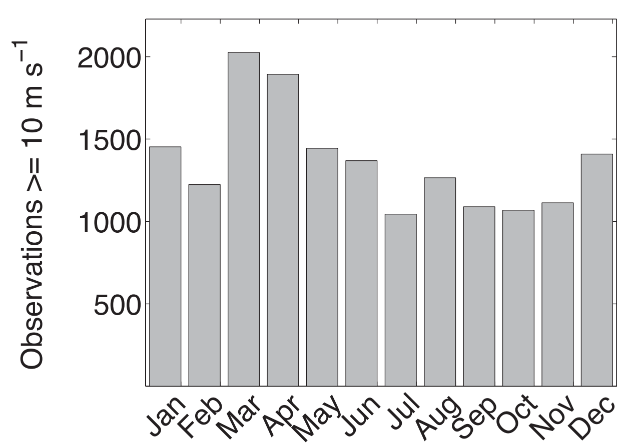

FIG. 8. Number of observations at KSLC with a sustained wind ≥ 10 m s^{-1} by month.

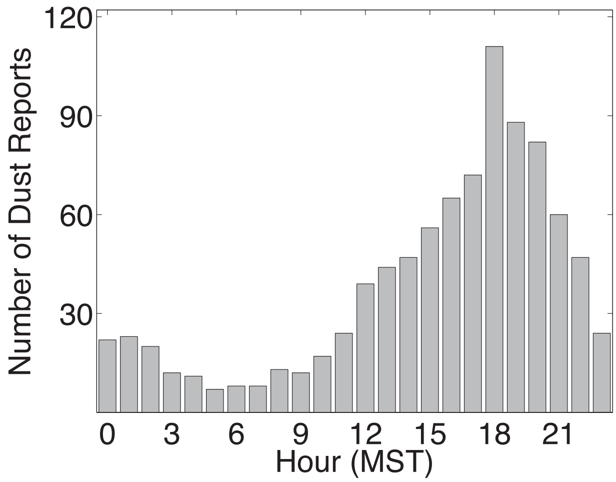

FIG. 9. Number of dust reports at KSLC by hour (MST).

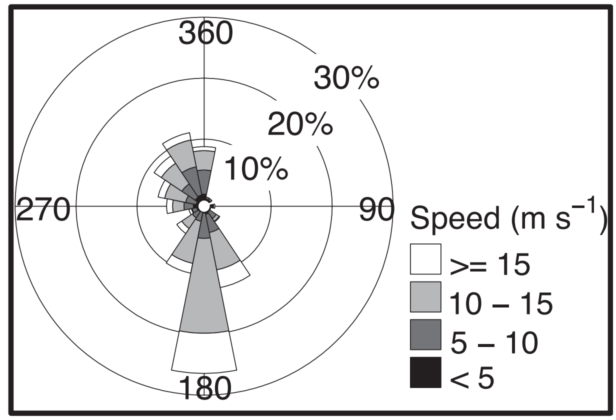

FIG. 11. Wind rose for KSLC dust reports.

morphology (Jewell and Nicoll 2011) and are capable of generating dust emissions and transport during favorable land surface conditions. In fact, dust was reported at KSLC within 3 h of the passage of 12 of the 25 strongest cold fronts identified by Shafer and Steenburgh (2008).

The mean sustained wind speed during dust reports at KSLC is 11.6 m s^{-1} (with a standard deviation of 4.0 m s^{-1}), slightly higher than the 8.5 and 9.29 m s^{-1} found by Holcombe et al. (1997) for Yuma, Arizona, and Blythe, California, respectively. Therefore, we use 10 m s^{-1} as an approximate threshold velocity for dust emissions and transport assuming favorable boundary layer and land surface conditions. At KSLC, reports of sustained winds $\geq$ 10 m s^{-1} are most common in March and April, with additional, but weaker maxima in August and January (Fig. 8). The March and April peak resembles the springtime peak in dust events and mean monthly total dust flux, but the lack of an autumn secondary maximum and winter minimum suggests that other factors related to the spatial scale of the strong winds (e.g., convective vs synoptically driven), and seasonal changes to vegetation, soil conditions, and soil moisture (Gillette 1999; Neff et al. 2008; Belnap et al. 2009) contribute to the seasonality of dust events and total dust flux.

Dust reports exhibit a strong diurnal cycle and are most common in the late afternoon and evening hours (Fig. 9), as observed in other regions (Jauregui 1989; N'Tchayi Mbourou et al. 1997). The frequency of sustained winds $\geq$ 10 m s^{-1} at KSLC is about 3 times as

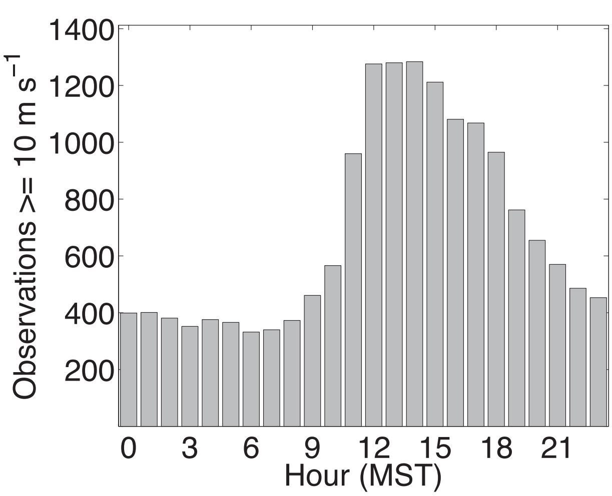

FIG. 10. Number of observations at KSLC with a sustained wind $\geq$ 10 m s^{-1} by hour (MST).

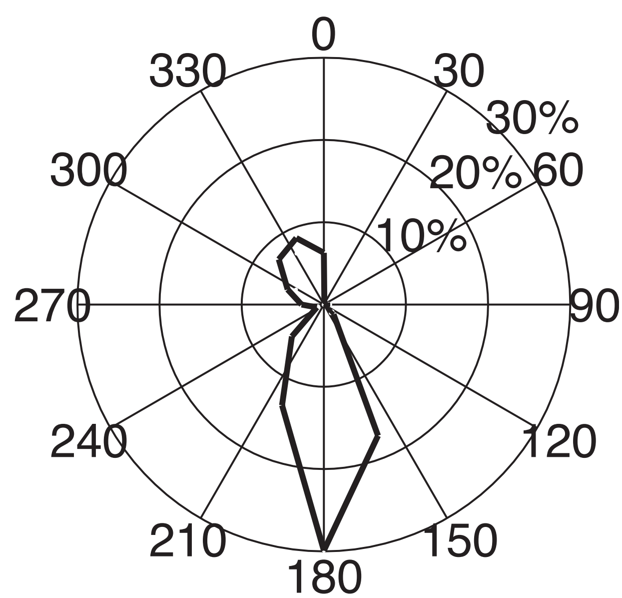

FIG. 12. Fraction (%) of total dust flux as a function of wind direction at KSLC.

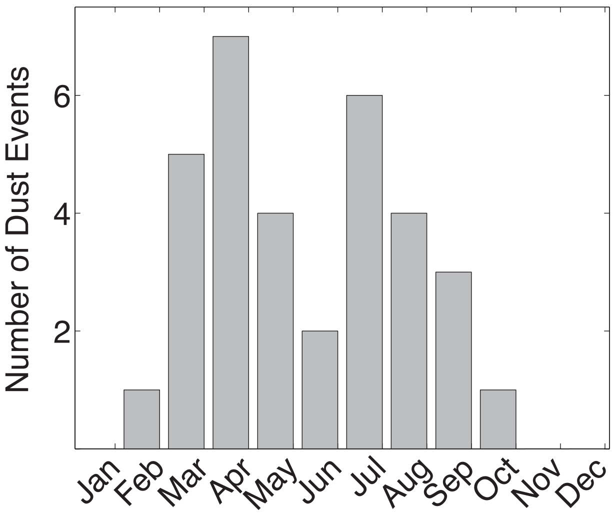

FIG. 13. Number of recent (2001–10) dust events at KSLC by month.

high in the afternoon as in the morning (Fig. 10), which is consistent with the development of the daytime convective boundary layer. The peak for sustained winds ≥ 10 m s^{-1} occurs at 1400 MST, 4 h earlier than the peak in dust reports, a likely consequence of the time needed for dust to travel from its sources to KSLC.

The frequency distribution of wind directions during dust events is bimodal, with peaks at southerly and north-northwesterly (Fig. 11). About 49% of the time, the wind is from the south-southwest through the south-southeast, and about 29% of the time the wind is north-westerly through northerly. Total dust flux is also greatest for winds from the south-southwest through south-southeast (Fig. 12).

TABLE 2. Date and primary synoptic conditions of recent (2001–10) dust events at KSLC. Abbreviations are AC (airmass convection), CF/BT (cold front or baroclinic trough entering Utah from the west or northwest), SF/BT (stationary or slowly moving front or baroclinic trough to the west or northwest of Utah), and O (other synoptic conditions).

Date	Synoptic conditions
23 Mar 2002	CF/BT
15 Apr 2002	CF/BT
1 Jun 2002	AC
16 Sep 2002	AC
1 Feb 2003	CF/BT
1 Apr 2003	SF/BT
2 Apr 2003	CF/BT
16 Sep 2003	O
28 Apr 2004	CF/BT
10 May 2004	CF/BT
9 Jul 2004	AC
17 Oct 2004	SF/BT
13 Mar 2005	O
13 Apr 2005	CF/BT
16 May 2005	CF/BT
22 Jul 2005	AC
30 Jul 2005	AC
19 May 2006	AC
19 Jul 2006	AC
26 Jul 2006	AC
29 Apr 2008	CF/BT
20 May 2008	CF/BT
27 Jul 2008	AC
31 Aug 2008	CF/BT
4 Mar 2009	CF/BT
21 Mar 2009	SF/BT
30 Jun 2009	AC
5 Aug 2009	AC
6 Aug 2009	CF/BT
30 Aug 2009	SF/BT
30 Sep 2009	CF/BT
30 Mar 2010	CF/BT
28 Apr 2010	CF/BT

b. Recent (2001–10) events

To classify dust events synoptically, we concentrate on 2001–10, which enables the use of modern reanalysis, satellite, and radar data. The monthly frequency distribution of the 33 dust events during this period resembles that of the long-term climatology except for a disproportionately high number of summer events (cf. Figs. 6 and 13).

The 33 recent dust events were classified subjectively into one of four groups depending on the primary synoptic conditions responsible for the dust emissions and transport: 1) airmass convection, 2) a cold front or baroclinic trough entering Utah from the west or northwest, 3) a stationary or slowly moving front or baroclinic trough to the west or northwest of Utah, and 4) other synoptic conditions (Table 2). The 11 (33%) events generated by airmass convection featured a thunderstorm, thunderstorm in the vicinity, or squall comment in the DS-3505 reports within an hour of the dust observation, and/or nearby convection in satellite or radar imagery, but no significant large-scale temperature gradient at 700 hPa. These events tended to be short lived (usually less than 2 h) and all occurred between mid-May and mid-September. For example, at 1600 MST 19 May 2006, KSLC observed a 5 m s^{-1} southerly wind but KMTX radar imagery showed strong convection just to the south (Fig. 14a; KSLC observation not shown). The passage of a convective outflow boundary (i.e., gust front; Wakimoto 1982) at KSLC at 1607 MST was accompanied by south-southwest winds of 24 m s^{-1} with gusts to 28 m s^{-1}, blowing dust, and a visibility of 6.4 km. By 1624 MST, blowing dust was no longer reported. A lack of strong flow and baroclinity at 700 hPa over northern Utah during this period further supports the classification of this event as airmass convection (Fig. 14b).

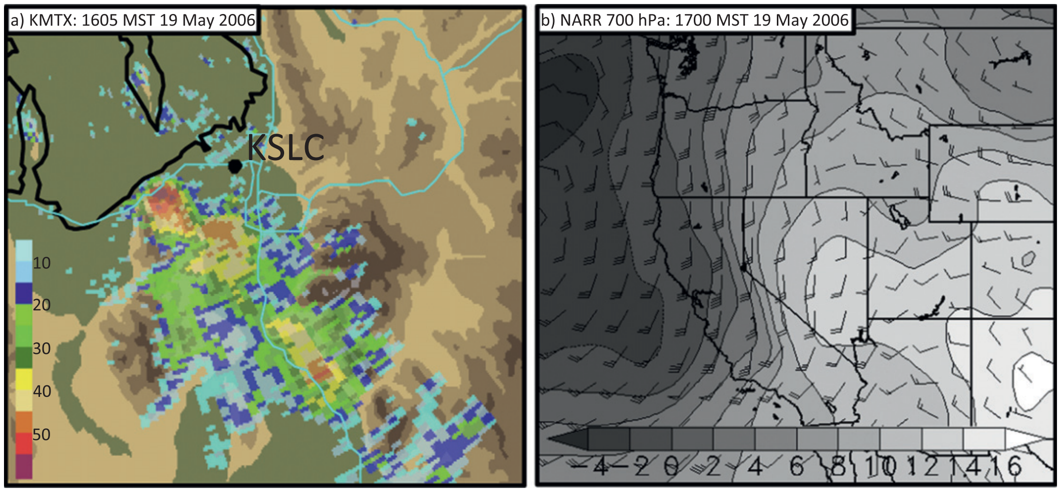

FIG. 14. Meteorological conditions during the 19 May 2006 dust event: (a) 1605 MST KMTX 0.5° radar reflectivity (dB*Z*; color scale at lower left) and topography (color filled with transitions at 1350, 1700, 2050, and 2400 m) and (b) 1700 MST NARR 700-hPa temperature (shaded; scale at bottom) and wind (full and half barb denote 2.5 and 5 m s^{-1}, respectively).

The 16 (48%) recent events produced by a cold front or baroclinic trough from the west or northwest featured at least one dust report at KSLC within 3 h of the cold-frontal or baroclinic-trough passage and a distinct frontal cloud band in visible satellite images. Thirteen of these events accompanied a cyclone over the Great Basin or adjoining northwestern United States as based on the existence of a closed 850-hPa isohypse at 30-m intervals, although dust reports at KSLC are concentrated around the timing of the accompanying frontal or baroclinic-trough passage [Fig. 15; see West and Steenburgh (2010) for a detailed case study of one of these 13 events (15 Apr 2002)]. Of the 16 events, 4 reported dust more than 3 h before the frontal passage, 8 reported dust within the 3 h before frontal passage, 14 reported dust within the 3 h after the frontal passage, and 2 reported dust more than 3 h after the frontal passage. A representative example occurred on 10 May 2004, when strong southerly–southwesterly flow ahead of a cold front and concomitant pressure trough produced several dust plumes that extended from southwest Utah to the Wasatch Front (Figs. 16a–c). Hourly and special aviation routine weather reports (METAR) archived by the MesoWest cooperative networks (Horel et al. 2002) show that dust was first reported at KSLC at 1655 MST, just before the frontal passage, which occurred between the 1655 and 1710 MST observations. The visibility was 8 km, with sustained winds of 18 m s^{-1} and wind gusts to 22 m s^{-1}. The dust-limited visibility dropped to 2.8 km following the frontal passage at 1710 MST, but by 1955 MST the visibility was greater than 10 km and dust was no longer reported. The entrainment of dust into the postfrontal air mass, combined with cold-frontal convergence, appeared to contribute to increased dust concentrations and decreased visibility during and immediately following frontal passage, as occurs in many events.

Strong prefrontal southerly flow within a deep convective boundary layer contributes to dust emissions and transport during these 16 cold-frontal or baroclinic-trough events. In comparison with a 21-day weighted climatology centered on the event dates, the NARR 700-hPa wind speed at KSLC at the time of the initial dust report during these events is skewed to much higher values, with the distribution of flow directions from 160°

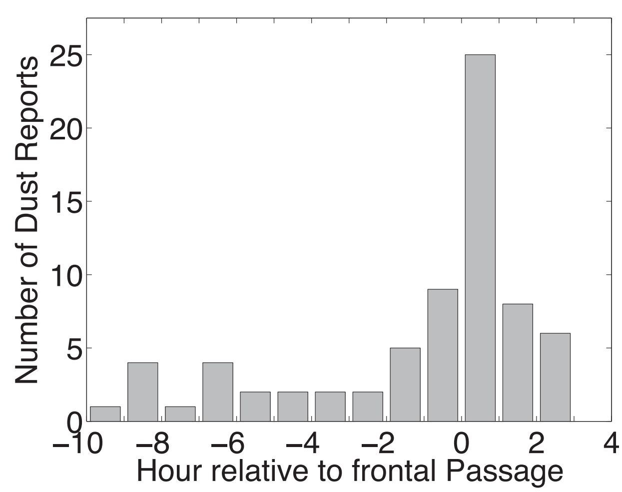

FIG. 15. Number of dust reports relative to frontal passage during recent (2001–10) dust events at KSLC with a cold-frontal or baroclinic-trough passage from the west or northwest.

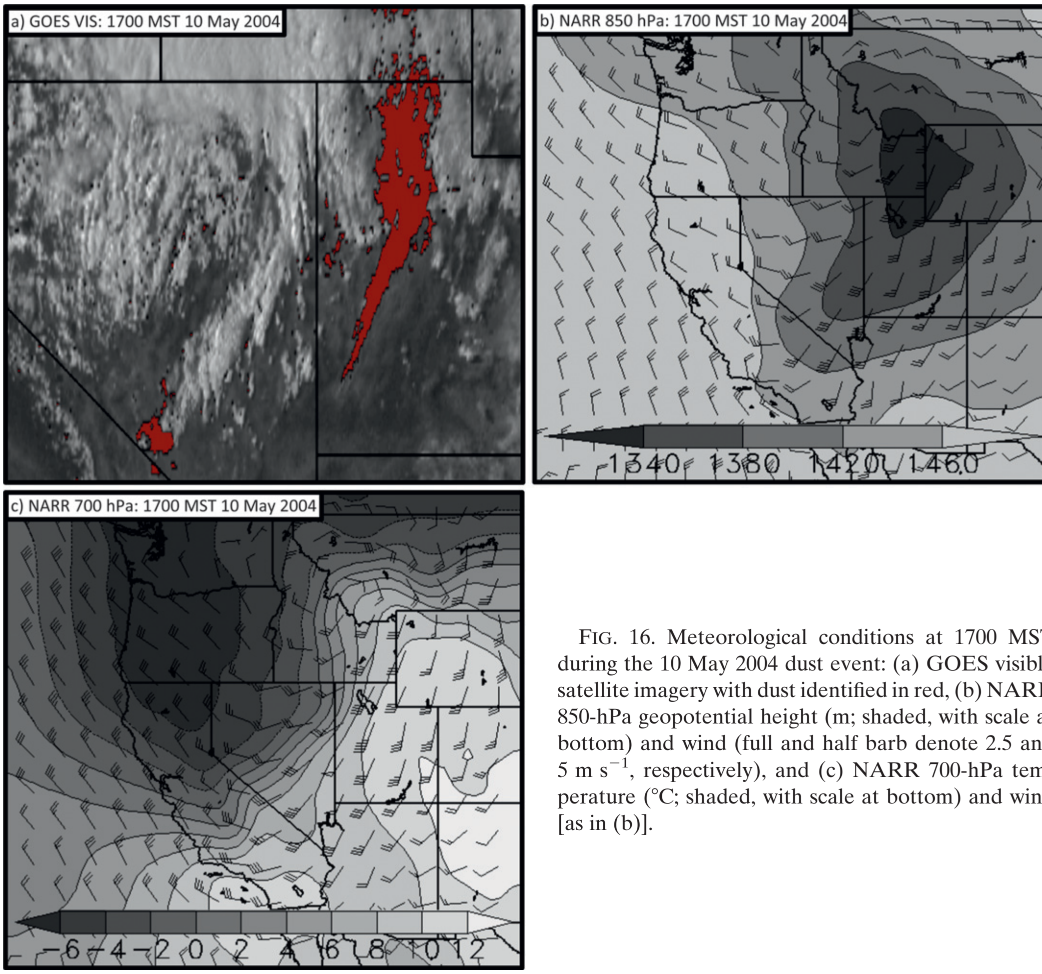

FIG. 16. Meteorological conditions at 1700 MST during the 10 May 2004 dust event: (a) GOES visible satellite imagery with dust identified in red, (b) NARR 850-hPa geopotential height (m; shaded, with scale at bottom) and wind (full and half barb denote 2.5 and 5 m s^{-1}, respectively), and (c) NARR 700-hPa temperature (°C; shaded, with scale at bottom) and wind [as in (b)].

to 260° (Figs. 17a,b). Maximum boundary layer depths on these dust-event days are skewed toward much higher values than climatological values, with a mode at 5000 m AGL (Fig. 17c). As shown by Shafer and Steenburgh (2008), strong winds within a deep convective boundary layer are common during strong Intermountain West cold-frontal events. As noted previously, of the 25 strong Intermountain West cold fronts identified at KSLC by Shafer and Steenburgh (2008, see their Table 1), 12 were accompanied by at least one dust report within 3 h of frontal passage. These results indicate that Intermountain West cold fronts and baroclinic troughs play an important role in regional dust emissions and transport. Further, the frequency of these cold-frontal and baroclinic-trough passages is greatest in the spring when dust-related radiative forcing can have its greatest impact on snowmelt (Painter et al. 2007).

Closely related to the cold-frontal and baroclinic-trough events noted above are four (18%) additional events that were produced by stationary or slowly moving fronts or baroclinic troughs to the west or northwest that remained upstream of KSLC for at least 24 h after the initial dust observation. During these events, dust emissions and transport occur in the strong southerly or southwesterly flow ahead of the frontal or baroclinic trough, as discussed above. One event (30 Aug 2009) may be erroneous since observer comments and satellite imagery indicate that smoke, not dust, likely reduced visibilities.

Two (6%) events were associated with other synoptic conditions. On 16 September 2003, KSLC reported dust in intensifying northwesterly flow as a surface trough and cyclone developed to the south. On 13 March 2005, dust was produced by strong winds following the passage of a cold front from the north. The large-scale evolution of this event resembled that found to contribute to two dust storms originating over the Black Rock Desert of northwestern Nevada by Lewis et al. (2011) and Kaplan et al. (2011).

The fraction of the total dust flux by event type clearly shows the dominant contribution of cold and

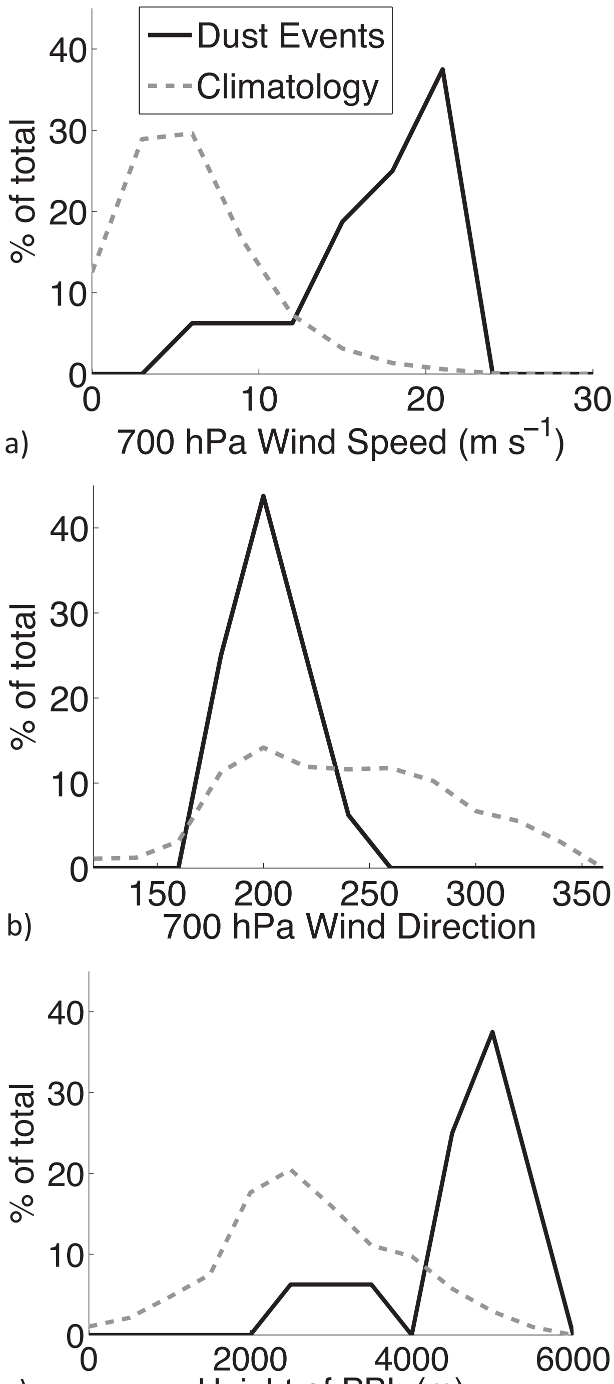

FIG. 17. Frequency of NARR (a) 700-hPa wind speed (m s^{-1}) at initial dust report, (b) 700-hPa wind direction (°) at initial dust report, and (c) maximum boundary layer depth (m AGL) at KSLC during recent (2001–10) dust events associated with a cold front or baroclinic trough entering Utah from the west or northwest (solid) relative to a weighted climatology that is based on 21 days centered on each event date (dashed).

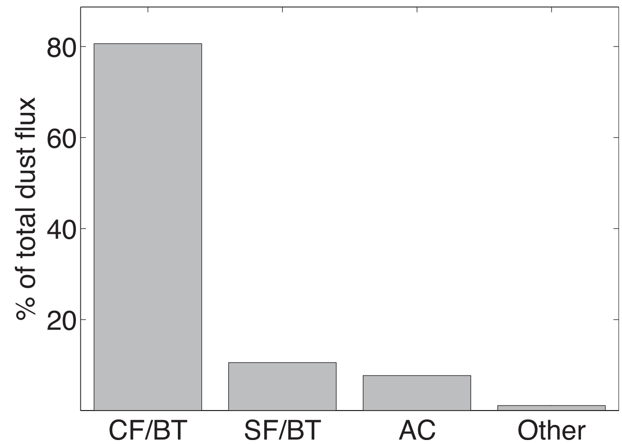

FIG. 18. Fraction (%) of total dust flux at KSLC by synoptic condition. Abbreviations are CF/BT (cold fronts and baroclinic troughs entering Utah from the west or northwest), SF/BT (stationary or slowly moving fronts and baroclinic troughs to the west or northwest of Utah), AC (airmass convection), and Other (other synoptic conditions).

quasi-stationary fronts and baroclinic troughs (81%; Fig. 18). Although airmass convection produces 11 of the 33 recent events, it only generates 8% of the total dust flux.

c. Dust emission sources

As described in section 2, we use a dust-retrieval algorithm applied to GOES imagery to identify the origin and orientation of dust plumes during the recent dust events. Given that plumes are not identifiable in some events because of cloud cover and/or an insufficient solar zenith angle, we include in this analysis the 33 recent (2001–10) events described above, as well as 61 additional events observed in DS-3505 reports from three weather stations in the surrounding region (Delta, Elko, and Pocatello; see Fig. 1) or identified in the authors' notes and annual Utah Avalanche Center reports. After applying the GOES dust-retrieval algorithm, 120 independent dust plumes were subjectively identified during 47 (50%) of the 94 dust events. Airmass convection and cold- or stationary-frontal or baroclinic-trough events with two or fewer dust observations most commonly were without visible plumes.

The origins of the 120 identifiable dust plumes are clustered primarily in low-elevation Late Pleistocene–Holocene alluvial environments in southern and western Utah and southern and western Nevada (Fig. 19). These include the Sevier Desert, Sevier Dry Lake Bed, Escalante Desert, Milford Valley, and West Desert of Utah and the Black Rock Desert, Carson Sink, and Great Basin and Mojave Deserts of Nevada. Since July of 2007, dust emissions from the Milford Valley likely include

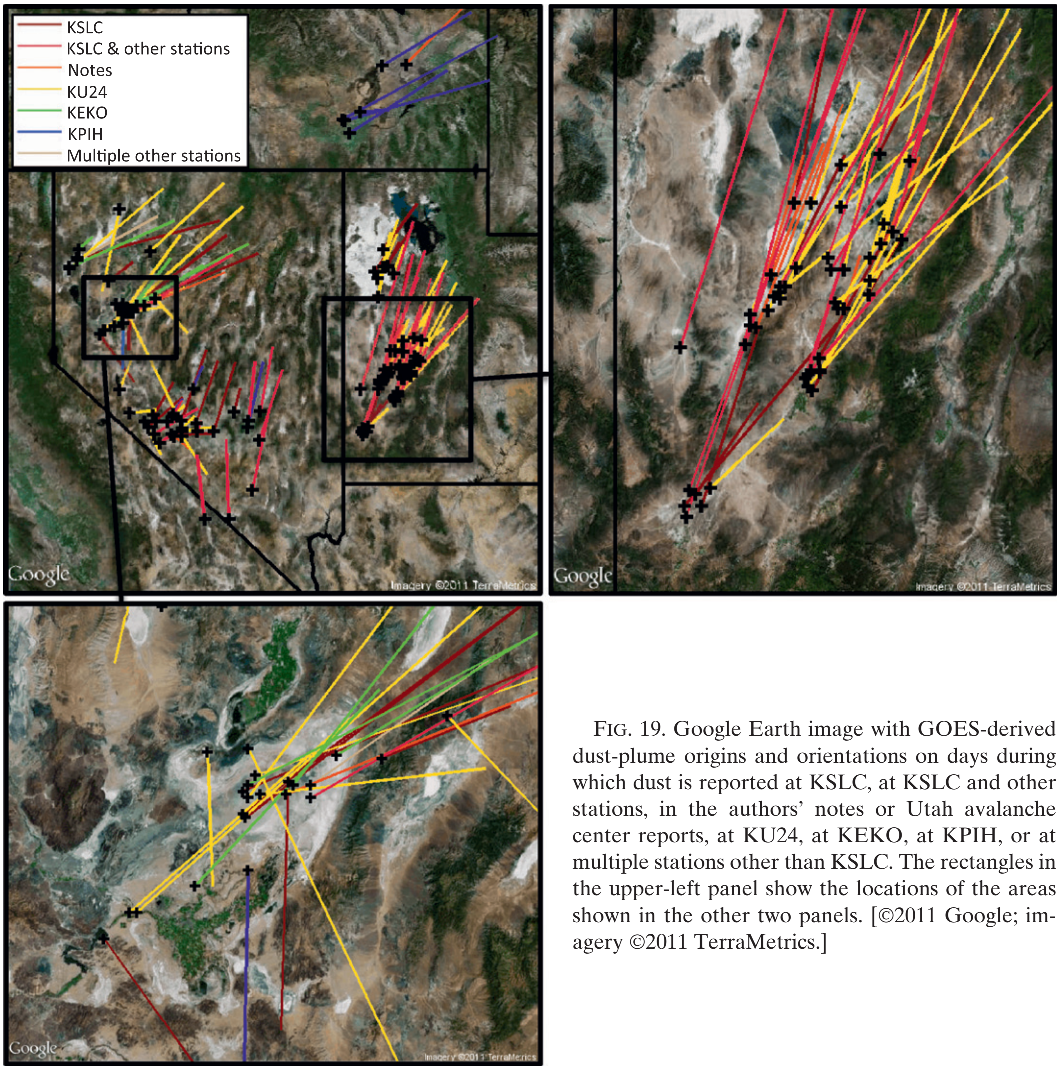

FIG. 19. Google Earth image with GOES-derived dust-plume origins and orientations on days during which dust is reported at KSLC, at KSLC and other stations, in the authors' notes or Utah avalanche center reports, at KU24, at KEKO, at KPIH, or at multiple stations other than KSLC. The rectangles in the upper-left panel show the locations of the areas shown in the other two panels. [©2011 Google; imagery ©2011 TerraMetrics.]

contributions from the Milford Flat fire scar (Miller et al. 2012). Plumes oriented toward KSLC, the Wasatch Front, and northern Utah originate primarily from southern and western Utah, consistent with what might be inferred from Figs. 11, 12, and 17 given the dominance of southerly flow. On average 2.6 plumes are identified on days with visible plumes, indicating that synoptic conditions that contribute to episodic dust events frequently activate multiple emissions sources. Because of obscuration, these results do not include dust plumes that form beneath existing plumes.

Not all of the dust identified in satellite imagery could be traced to a clear origin as there were 11 examples of broad areal dust emissions. The dust in a majority of these examples originated over western Nevada and moved to the southeast, but there was one event with areal dust emissions over central Utah and another with areal dust emissions over the Snake River Plain.

4. Conclusions

Episodic dust events contribute to hazardous air quality and dust loading of the snowpack along Utah's Wasatch Front and adjoining region. Surface weather observations from the Salt Lake City International Airport show that these dust events occur throughout the 1930–2010 study period, with considerable interannual variability. The annual dust-event frequency and total dust flux exhibit a general decline during the study period that is broadly consistent with decreased mass sedimentation rates related to dust deposition in alpine lakes of western Colorado that followed passage of the 1934 Taylor Grazing Act (e.g., Neff et al. 2008).

The distributions of monthly dust-event frequency and mean total dust flux are bimodal, with a primary peak in spring (April) and a secondary peak in autumn

(September) that closely resemble the monthly frequency of strong Intermountain West cold fronts and Intermountain West cyclones (Shafer and Steenburgh 2008; Jeglum et al. 2010). The total dust flux is greatest during periods of strong southerly winds, with a weaker secondary maximum associated with flow from the northwest.

An analysis of 33 recent (2001–10) events shows that 11 were associated with airmass convection, 16 were associated with a cold front or baroclinic trough entering Utah from the west or northwest, 4 were associated with a stationary or slowly moving front or baroclinic trough west of Utah, and 2 were associated with other synoptic patterns. The fraction of total dust flux observed at KSLC is strongly dominated by cold- and quasi-stationary-frontal or baroclinic-trough events, many of which feature strong southerly winds in a deep convective boundary layer.

Subjective analysis of dust plumes identified using GOES imagery indicates that regional dust emission sources during these episodic dust events are clustered primarily in low-elevation Late Pleistocene–Holocene alluvial environments in southern and western Utah and southern and western Nevada. Areas with the greatest concentration of emission sources include the Sevier Desert, Sevier Dry Lake Bed, Escalante Desert, Milford Valley, and West Desert of Utah and the Black Rock Desert, Carson Sink, and Great Basin and Mojave Deserts of Nevada.

These findings are based on the analysis of episodic dust events identified in conventional meteorological observations. Dust emissions, transport, and deposition during other periods may also influence snowpack, soil, and lake-sediment composition over the region. In addition, an important aspect of episodic dust events not investigated here is land surface variability and its contribution to enhanced dust fluxes under climate change (Munson et al. 2011; Okin et al. 2011). Improved understanding of soil moisture, vegetation, and anthropogenic disturbance (e.g., Neff et al. 2005; Reynolds et al. 2007; Belnap et al. 2009; Miller et al. 2012) may help to improve the prediction of these events. Moreover, mitigation efforts in the areas of frequent emissions identified above, especially those in southern and western Utah, may reduce the frequency and severity of episodic dust events over the Wasatch Front and adjoining region. Such mitigation efforts are currently being investigated by regional and federal land and water management agencies.

Acknowledgments. We thank Trevor Alcott for his contributions to the KSLC dust-event climatology and Paul Jewell for assisting with the identification of dust emission sources. John Lewis and two anonymous referees provided reviews that helped to improve the manuscript. We gratefully acknowledge the provision of datasets, software, and/or computer time and services by NCEP, NCAR, Unidata, the Center for Ocean–Land–Atmosphere Studies, and the University of Utah Center for High Performance Computing. This research was supported by National Science Foundation Grant AGS-0627937, NASA Grant NNX10AO97G, and USDA Forest Service Agreement 10-PA-11041914-045. Any opinions, findings, and conclusions or recommendations expressed in this paper are those of the authors and do not necessarily reflect the views of the National Science Foundation, NASA, or the USDA Forest Service.

REFERENCES

Bear West Consulting Team, 1999: Salt Lake City Watershed Management Plan. Salt Lake City Department of Public Utilities, 129 pp. [Available online at http://www.slcclassic.com/utilities/PDF%20Files/slcwatershedmgtplan.pdf.]

Belnap, J., R. L. Reynolds, M. C. Reheis, S. L. Phillips, F. E. Urban, and H. L. Goldstein, 2009: Sediment losses and gains across a gradient of livestock grazing and plant invasion in a cool, semi-arid grassland, Colorado Plateau, USA. *Aeolian Res.,* **1,** 27–43.

Brazel, A. J., 1989: Dust and climate in the American southwest. *Paleoclimatology and Paleometeorology: Modern and Past Patterns of Global Atmospheric Transport,* M. Leinen and M. Sarnthein, Eds., Kluwer Academic, 65–96.

——, and W. G. Nickling, 1986: The relationship of weather types to dust storm generation in Arizona (1965–1980). *Int. J. Climatol.,* **6,** 255–275.

——, and ——, 1987: Dust storms and their relation to moisture in the Sonoran–Mojave desert region of the south-western United States. *J. Environ. Manage.,* **24,** 279–291.

Carlson, T. N., 1979: Atmospheric turbidity in Saharan dust outbreaks as determined by analyses of satellite brightness data. *Mon. Wea. Rev.,* **107,** 322–335.

Changery, M. J., 1983: A dust climatology of the western United States. National Climatic Data Center Tech. Rep. NUREG/CR-3211, 44 pp.

Fairlie, T. D., D. J. Jacob, and R. J. Park, 2007: The impact of transpacific transport of mineral dust in the United States. *Atmos. Environ.,* **41,** 1251–1266.

Flanner, M. G., C. S. Zender, P. G. Hess, N. M. Mahowald, T. H. Painter, V. Ramanathan, and P. J. Rasch, 2009: Springtime warming and reduced snow cover from carbonaceous particles. *Atmos. Chem. Phys.,* **9,** 2481–2497.

Gebhart, K. A., S. M. Kreidenweis, and W. C. Malm, 2001: Back-trajectory analyses of fine particulate matter measured at Big Bend National Park in the historical database and the 1996 scoping study. *Sci. Total Environ.,* **276,** 185–204.

Gillette, D. A., 1988: Threshold friction velocities for dust production for agricultural soils. *J. Geophys. Res.,* **93,** 12 645–12 662.

——, 1999: A qualitative geophysical explanation for hot spot dust emitting source regions. *Contrib. Atmos. Phys.,* **72,** 67–77.

——, J. Adams, A. Endo, D. Smith, and R. Kihl, 1980: Threshold velocities for input of soil particulates into the air by desert soils. *J. Geophys. Res.,* **85,** 5621–5630.

Glickman, T., Ed., 2000: *Glossary of Meteorology*. 2nd ed. Amer. Meteor. Soc., 855 pp.

Gorrell, M., 2011: Ski season was Utah's 2nd-busiest. *The Salt Lake Tribune,* 5 July 2011. [Available online at http://www.sltrib.com/sltrib/money/52134347-79/ski-utah-season-2010-11.html.csp.]

Goudie, A. S., and N. J. Middleton, 2001: Saharan dust storms: Nature and consequences. *Earth Sci. Rev.,* **56,** 197–204.

Hall, F. F., Jr., 1981: Visibility reductions from soil dust in the western U.S. *Atmos. Environ.,* **15,** 1929–1933.

Holcombe, T. L., T. Ley, and D. A. Gillette, 1997: Effects of prior precipitation and source area characteristics on threshold wind velocities for blowing dust episodes, Sonoran Desert 1948–78. *J. Appl. Meteor.,* **36,** 1160–1175.

Horel, J., and Coauthors, 2002: Mesowest: Cooperative mesonets in the western United States. *Bull. Amer. Meteor. Soc.,* **83,** 211–225.

Husar, R. B., and Coauthors, 2001: Asian dust events of April 1998. *J. Geophys. Res.,* **106,** 18 317–18 330.

Jaffe, D., and Coauthors, 1999: Transport of Asian air pollution to North America. *Geophys. Res. Lett.,* **26,** 711–714.

Jauregui, E., 1989: The dust storms of Mexico City. *Int. J. Climatol.,* **9,** 169–180.

Jeglum, M. E., W. J. Steenburgh, T. P. Lee, and L. F. Bosart, 2010: Multi-reanalysis climatology of Intermountain cyclones. *Mon. Wea. Rev.,* **138,** 4035–4053.

Jewell, P. W., and K. Nicoll, 2011: Wind regimes and Aeolian transport in the Great Basin, U.S.A. *Geomorphology,* **129,** 1–13.

Kaplan, M. L., R. K. Vellore, J. M. Lewis, and M. Young, 2011: The role of unbalanced mesoscale circulations in dust storms. *J. Geophys. Res.,* **116,** D23101, doi:10.1029/2011JD016218.

Lewis, J. M., M. L. Kaplan, R. Vellore, R. M. Rabin, J. Hallett, and S. A. Cohn, 2011: Dust storm over the Black Rock Desert: Larger-scale dynamic signatures. *J. Geophys. Res.,* **116,** D06113, doi:10.1029/2010JD014784.

Lott, N., R. Baldwin, and P. Jones, 2001: The FCC integrated surface hourly database: A new resource of global climate data. National Climatic Data Center Tech. Rep. 2001-01, 42 pp. [Available online at http://www1.ncdc.noaa.gov/pub/data/inventories/ish-tech-report.pdf.]

Mesinger, F., and Coauthors, 2006: North American Regional Reanalysis. *Bull. Amer. Meteor. Soc.,* **87,** 343–360.

Miller, M. E., M. A. Bowker, R. L. Reynolds, and H. L. Goldstein, 2012: Post-fire land treatments and wind erosion—Lessons from the Milford Flat Fire, UT, USA. *Aeolian Res.,* doi:10.1016/j.aeolia.2012.04.001, in press.

Munson, S. M., J. Belnap, and G. S. Okin, 2011: Responses of wind erosion to climate-induced vegetation changes on the Colorado Plateau. *Proc. Natl. Acad. Sci. USA,* **108,** 3854–3859.

NCDC, 2008: Data documentation for data set 3505 (DSI-3505): Integrated surface data. National Climatic Data Center, 119 pp. [Available online at http://www1.ncdc.noaa.gov/pub/data/documentlibrary/tddoc/td3505.doc.]

Neff, J. C., R. L. Reynolds, J. Belnap, and P. Lamothe, 2005: Multi-decadal impacts of grazing on soil physical and biogeochemical properties in southeast Utah. *Ecol. Appl.,* **15,** 87–95.

——, and Coauthors, 2008: Increasing eolian dust deposition in the western United States linked to human activity. *Nat. Geosci.,* **1,** 189–195.

Nicholson, S., 2000: Land surface processes and Sahel climate. *Rev. Geophys.,* **38,** 117–139.

Nickling, W. G., and A. J. Brazel, 1984: Temporal and spatial characteristics of Arizona dust storms (1965–1980). *Int. J. Climatol.,* **4,** 645–660.

N'Tchayi Mbourou, G., J. J. Bertrand, and S. E. Nicholson, 1997: The diurnal and seasonal cycles of wind-borne dust over Africa north of the equator. *J. Appl. Meteor.,* **36,** 868–882.

OFCM, 2005: Federal Meteorological Handbook No. 1: Surface weather observations and reports. Office of the Federal Coordinator for Meteorological Services and Supporting Research FCM-H1-2005, 104 pp. [Available online at http://www.ofcm.gov/fmh-1/fmh1.htm.]

Okin, G. S., and Coauthors, 2011: Dust: Small-scale processes with global consequences. *Eos, Trans. Amer. Geophys. Union,* **92,** 241, doi:10.1029/2011EO290001.

Orgill, M. M., and G. A. Sehmel, 1976: Frequency and diurnal variation of dust storms in the contiguous U.S.A. *Atmos. Environ.,* **10,** 813–825.

Painter, T. H., and Coauthors, 2007: Impact of disturbed desert soils on duration of mountain snow cover. *Geophys. Res. Lett.,* **34,** L12502, doi:10.1029/2007GL030284.

——, J. S. Deems, J. Belnap, A. F. Hamlet, C. C. Landry, and B. Udall, 2010: Response of Colorado River runoff to dust radiative forcing in snow. *Proc. Natl. Acad. Sci. USA,* **107,** 17 125–17 130.

Pope, C. A., D. V. Bates, and M. E. Raizenne, 1995: Health effects of particulate air pollution: Time for reassessment? *Environ. Health Perspect.,* **103,** 472–480.

Prospero, J. M., and P. J. Lamb, 2003: African droughts and dust transport to the Caribbean: Climate change implications. *Science,* **302,** 1024–1027.

Qian, W., L. Quan, and S. Shi, 2002: Variations of the dust storm in China and its climatic control. *J. Climate,* **15,** 1216–1229.

Ramanathan, V., P. J. Crutzen, J. T. Kiehl, and D. Rosenfeld, 2001: Aerosols, climate, and the hydrological cycle. *Science,* **294,** 2119–2124.

Reynolds, R., J. Belnap, M. Reheis, P. Lamothe, and F. Luiszer, 2001: Aeolian dust in Colorado Plateau soils: Nutrient inputs and recent change in source. *Proc. Natl. Acad. Sci. USA,* **98,** 7123–7127.

——, and Coauthors, 2007: Dust emissions from wet and dry playas in the Mojave Desert, USA. *Earth Surf. Processes Landforms,* **32,** 1811–1827.

——, J. S. Mordecai, J. G. Rosenbaum, M. E. Ketterer, M. K. Walsh, and K. A. Moser, 2010: Compositional changes in sediments of subalpine lakes, Uinta Mountains (Utah): Evidence for the effects of human activity on atmospheric dust inputs. *J. Paleolimnol.,* **44,** 161–175.

Ritchie, E. A., K. M. Wood, D. S. Gutzler, and S. R. White, 2011: The influence of eastern Pacific tropical cyclone remnants on the southwestern United States. *Mon. Wea. Rev.,* **139,** 192–210.

Sanders, F., 1999: A proposed method of surface map analysis. *Mon. Wea. Rev.,* **127,** 945–955.

Shafer, J. C., and W. J. Steenburgh, 2008: Climatology of strong Intermountain cold fronts. *Mon. Wea. Rev.,* **136,** 784–807.

Shao, Y., and J. Wang, 2003: A climatology of northeast Asian dust events. *Meteor. Z.,* **12,** 187–196.

——, and Coauthors, 2003: Northeast Asian dust storms: Real-time numerical prediction and validation. *J. Geophys. Res.,* **108,** 4691, doi:10.1029/2003JD003667.

Song, Z., J. Wang, and S. Wang, 2007: Quantitative classification of northeast Asian dust events. *J. Geophys. Res.,* **112,** D04211, doi:10.1029/2006JD007048.

Steenburgh, W. J., and T. I. Alcott, 2008: Secrets of the ''Greatest Snow on Earth.'' *Bull. Amer. Meteor. Soc.,* **89,** 1285–1293.

Stout, J. E., 2001: Dust and environment in the southern high plains of North America. *J. Arid Environ.,* **47,** 425–441.

Swap, R., S. Ulanski, M. Cobbett, and M. Garstang, 1996: Temporal and spatial characteristics of Saharan dust outbreaks. *J. Geophys. Res.,* **101,** 4205–4220.

Tanaka, T. Y., and M. Chiba, 2006: A numerical study of the contributions of dust source regions to the global dust budget. *Global Planet. Change,* **52,** 88–104.

VanCuren, R. A., and T. A. Cahill, 2002: Asian aerosols in North America: Frequency and concentration of fine dust. *J. Geophys. Res.,* **107,** 4804, doi:10.1029/2002JD002204.

Wakimoto, R. M., 1982: The life cycle of thunderstorm gust fronts as viewed with Doppler radar and rawinsonde data. *Mon. Wea. Rev.,* **110,** 1060–1082.

West, G. L., and W. J. Steenburgh, 2010: Life cycle and mesoscale frontal structure of an Intermountain cyclone. *Mon. Wea. Rev.,* **138,** 2528–2545.

Wheaton, E. E., and A. K. Chakravarti, 1990: Dust storms in the Canadian prairies. *Int. J. Climatol.,* **10,** 829–837.

WMO, 2009: Manual on codes: International codes. Vol. I.1 (Part A—Alphanumeric codes), WMO-No. 306, 462 pp. [Available online at http://www.wmo.int/pages/prog/www/WMOCodes/VolumeI1.html#VolumeI1.]

Yasunori, K., and M. Masao, 2002: Seasonal and regional characteristics of dust event in the Taklimakan Desert. *J. Arid Land Studies,* **11,** 245–252.

Zhao, T., S. Ackerman, and W. Guo, 2010: Dust and smoke detection for multi-channel imagers. *Remote Sens.,* **2,** 2347–2368.

Zobeck, T. M., D. W. Fryrear, and R. D. Pettit, 1989: Management effects on wind-eroded sediment and plant nutrients. *J. Soil Water Conserv.,* **44,** 160–163.